Title page

Characteristics of Stable Hydrogen and Oxygen Isotopes in Precipitation over the Jiaolai Plain, and its Water Vapor Sources

Ying Wang [a], Bu-li Cui*[a,b], Dong-sheng Li [a], Ya-Xuan Wang [a]

[a] *School of Resources and Environmental Engineering, Ludong University, Yantai 264025, China*

[b] *State Key Laboratory of Loess and Quaternary Geology, Institute of Earth Environment, Chinese Academy of Sciences, Xi'an 710061, China*

*Corresponding author:

Bu-Li Cui, School of Resources and Environmental Engineering, Ludong University, No. 186 Hongqizhong Street, Yantai, Shandong, 264025, China. Tel: +86-535-18953511817, Email: cuibuli@163.com

Abstract: Precipitation is the sole input of regional water resources in mountainous or hilly areas that are not traversed by large rivers. A prerequisite for using isotopic techniques to study the regional water cycle of a mountainous area is to examine the stable isotopic composition of its precipitation. The findings are of great significance for in-depth understanding of the water-cycle processes. In this study, each event of precipitation was sampled and used to investigate the characteristics of stable hydrogen and oxygen isotopes (δ^2H and $\delta^{18}O$, respectively) in precipitation on the Jiaolai Plain and its surrounding areas. NCEP/NCAR data was used for the wind speed and direction, relative humidity, and precipitable amount in the study area during the sampling period. The water vapor sources of precipitation over the plain were revealed through a comparative analysis of seasonal variations in precipitation isotopes, between the Global Network of Isotopes in Precipitation (GNIP) stations located along different vapor transport paths. The results showed that the local meteoric water line (LMWL) was $\delta^2H = 6.38\ \delta^{18}O + 0.72$, with a gradient less than 8. This indicated that the precipitation process was affected by non-equilibrium evaporation occurred when the drops fell below the cloud base. Significant temperature and amount effects existed in the $\delta^{18}O$ of precipitation, although the altitude effect was not significant. The water vapor source of the precipitation was controlled predominantly by the East Asian Monsoon from June to September, with the main source being evaporation from the adjacent Pacific Ocean. The plain was controlled by Westerlies from October through May, with the predominant vapor source being local evaporation. Water vapor from the polar region had minimal impact. During the sampling period, water vapor brought by Typhoon Lekima produced heavy precipitation on the plain from August 11–13, 2019. There was a significant depletion of $\delta^{18}O$ in the precipitation at that time, indicating the existence of the "cloud–rain zonal effect." These findings can serve as the basis for studying surface water–groundwater–seawater transformations, and the water-cycle in the Jiaolai Plain, and provide support for the rational use of water resources there.

Keywords: Stable isotopes; precipitation; water vapor sources; the Jiaolai Plain

1. Introduction

Precipitation is a critical component of the water-cycle processes, and the main source of terrestrial water resources [1]. In hilly areas not traversed by big rivers, precipitation is the only input of regional water resources. Studying the water vapor sources is a prerequisite for understanding the regional water-cycle and ensuring the rational use of water resources [2]. The composition of stable hydrogen and oxygen isotopes (δ^2H and $\delta^{18}O$, respectively) in precipitation is related to its water vapor sources and meteorological conditions, and responds sensitively to environmental changes. These characteristics make the δ^2H and $\delta^{18}O$ of precipitation an effective tool for studying climate change and hydrological processes, as well as a tracer for the sources and development of various waterbodies [3-6]. For these reasons, δ^2H and $\delta^{18}O$ in water are often referred to as its "fingerprint" or "DNA," and have become natural tracers for the water-cycle and climatic conditions [7-11].

For example, Pang et al.[12] analyzed the isotopic composition of precipitation at two high-altitude stations on the Tianshan Mountains in northwestern China, and confirmed the impacts of below-cloud evaporation and water recycling on the formation and isotopic composition of precipitation under arid climatic conditions. Using the 1968–2010 isotopic data for precipitation in the Hubbard Brook Experimental Forest, Puntsag et al. [2] found that the region's precipitation was affected by the North Atlantic Oscillation, Arctic sea ice decline, and intrusion of polar air. After analyzing the isotopic characteristics of precipitation in Thailand, and combining that with the results of atmospheric circumfluence and back-trajectory simulations, Wei et al. [13] concluded that the isotopic ratio of precipitation there was controlled by local evaporation, and that precipitation was significantly affected by large-scale convection. Kong et al. [4] analyzed the precipitation isotopic data of 68 stations in China,

and divided the country into five zones – Westerlies, Arctic, Northeast, Pacific, and Tibetan Plateau – based on their main water vapor sources. They also determined the spatiotemporal variations in the stable precipitation isotopes and deuterium excess (d-excess) of each zone. All the aforementioned studies reflect the value of using the $\delta^{2}H$ and $\delta^{18}O$ of precipitation to study water vapor sources and track the atmospheric water vapor cycle at various scales.

The Jiaolai Plain is located on the eastern margin of the mid-latitude Eurasian continent, and the central–eastern portion of the Shandong Peninsula in China (Fig.1). It is one of the core areas driving the economic development of Shandong Province [14-15]. Located in the eastern hilly areas of the Shandong Peninsula, it is not traversed by any large river, and precipitation is the region's only source of fresh water [16]. The implication of this is that the spatiotemporal distribution of precipitation directly affects the industrial and agricultural productivity of the plain. There has been an increase in the frequency and duration of drought events on the plain since the 1980s, resulting in a shortage of surface water resources. In addition to over-exploitation of the groundwater there by agricultural production, a large-scale negative funnel zone has also appeared in the groundwater level [17]. This has led to a series of serious geological and environmental problems in some areas, including land subsidence, seawater intrusions, ecological degradation, reduction in agricultural production, and exacerbation of endemic diseases [18-20]. The severe impact of these issues on the sustainable socioeconomic development of the area has attracted the attention of scholars and government, resulting in many studies being conducted. These researches have mainly focused on the formation of the groundwater funnel, the cause and exchange rate of seawater intrusions, pollution of the groundwater bodies, and evaluation of the water resources [20-23].

However, research on precipitation, the only input, is relatively lacking. In fact, there has been no research on the isotopic characteristics of the precipitation on the Jiaolai Plain and its surrounding areas,

nor its water vapor sources. This has imposed certain limitations on research into the transformation of the regional waterbodies and water-cycle, as well as preventing in-depth development of related research on regional ecological degradation, groundwater pollution, and investigations into the causes of endemic diseases.

Therefore, based on the above considerations, the Jiaolai Plain was taken as the study area, with event precipitation samples collected from 6 meteorological stations there. The main aims of this study were: (1) to explore the spatiotemporal variations in the precipitation isotopes of the study area; (2) to ascertain the environmental effects of these precipitation isotopes; and (3) to examine the water vapor sources of the precipitation in the study area, and its response to typhoon events. The findings can serve as basic data for research on surface water–groundwater–seawater transformations and the water-cycle of the plain, and inform strategies for the rational utilization of water resources there.

2. Background of the Jiaolai Plain

The Jiaolai Plain (or Jiaolai Valley) is located between the Luzhong Mountains and Jiaodong Hills (118°34′55″–120°40′15″ E, 35°38′38″–37°23′43″ N). Stretching 30–80 km from east to west, and reaching the Laizhou and Jiaozhou Bays to the north and south, respectively, the altitude of most of the plain is less than 50 m (Fig. 1). It was formed by the impacts of the Wei, Dagu, and Jiaolai Rivers, which had developed in the hilly areas on both sides (Fig. 1). Since the intention of this study was to analyze the isotopic characteristics of precipitation on the plain at the basin scale, the scope was expanded to include the watersheds of the Wei, Dagu, and Jiaolai Rivers (Fig. 1). The final study area covered a basin area of 17,762.22 km^2.

The study area has an oceanic, warm, and temperate monsoon climate with an annual average temperature of 11.8–12.9°C. The total annual precipitation, at approximately 670 mm, has an uneven

spatiotemporal distribution. It is mostly concentrated from June to August (approximately 60–65% of the annual precipitation) and decreases progressively from southeast to northwest [24]. The annual average evaporation is 1,665.1–2,158.1 mm, and the relative humidity is 68–72%. The annual frost-free period lasts 190–210 days, and the maximum frost depth is 40–50 cm. The Wei, Dagu, and Jiaolai Rivers are the largest rivers in the study area, with annual average runoffs of 14.45×10^8, 6.61×10^8, and 1.98×10^8 m^3, respectively. All the rivers are rain-sourced, and the flooding season is from June to September.

3. Methods

3.1 Collection and testing of precipitation samples

After taking into account the distributions of the topographical and altitudinal characteristics of the study area, 6 precipitation collection points were set up at the following meteorological bureaus: Changyi, Gaomi, Laixi, Laizhou, Pingdu, and Wulian (Fig. 1). A total of 254 precipitation samples were collected between October 2018 and September 2019, including 232 rainfall samples and 22 snowfall samples. During the sampling period, the amount of precipitation and the temperature during precipitation were observed simultaneously. δ^2H and $\delta^{18}O$ in the precipitation samples were measured using a Los Gatos Research liquid water liquid water isotope analyzer (IWA-45-EP) at the Northwest Agriculture and Forestry University, with VSMOW as the standard sample. The measurement accuracies for δ^2H and $\delta^{18}O$ were ±0.5‰ and ±0.2‰, respectively.

3.2 Research methods

The temperature, precipitation amount, and altitude effects were selected for analyzing the environmental effects of precipitation isotopes on the Jiaolai Plain [8,25-26]. The reanalysis data of the United States' National Centers for Environmental Prediction / National Center for Atmospheric Research (NCEP/NCAR) were used for the wind speed and direction, relative humidity, and precipitable

amount over the study area and its surrounding areas, at the geopotential height of 850 hPa, during the sampling period (October 2018 to September 2019). The spatial resolution of the data was 2.5° × 2.5° (data source: http://www.cdc.noaa.gov/cdc/reanalysis/). The purpose was to determine the precipitation source of the plain, and the characteristics of the water vapor migration path.

At the same time, the results for the water vapor sources were verified through a comparative analysis with the characteristics of seasonal variations in precipitation isotopes along different precipitation paths on the Global Network of Isotopes in Precipitation (GNIP) website. The stations included Urumqi, Baotou, Shijiazhuang, and Tokyo (Japan), from west to east, and Hong Kong, Nanjing, and Qiqihar, from south to north. Among these, Hong Kong is located in southeastern China and is affected by the East Asian Monsoon; Urumqi is located in northwest China and is affected by the Westerlies; for Baotou and Shijiazhuang (northwest of the study area), Tokyo (east of the study area), Nanjing (south of the study area), and Qiqihar (north of the study area), the wet and dry seasons are affected by the East Asian Monsoon and the Westerlies, respectively (Fig. 1)[27-28]. Data on the stations' precipitation isotopes were downloaded from the GNIP website (http://www.iaea.org/water) [29].

4. Results and discussion

4.1 Characteristics of precipitation isotopes

The $\delta^{2}H$ of precipitation on the Jiaolai Plain ranged from -89.76‰ to -0.54‰ (average: -34.43‰), and the $\delta^{18}O$ was between -13.85‰ and -0.05‰ (average: -5.51‰) (Fig. 2). These values are within the fluctuation range of $\delta^{2}H$ and $\delta^{18}O$ for China's precipitation, which is -280.0‰–+24.0‰ and -35.5‰–+2.5‰, respectively [30]. The temporal distributions of $\delta^{2}H$ and $\delta^{18}O$ exhibited a similar pattern, with both presenting a bimodal shape ("M" type). There was a gradual enrichment from January to May, followed by a gradual depletion from May to August, another gradual enrichment from August to

September, and another gradual depletion from September to December (Fig. 2). The overall characteristics followed the seasonal variations, being low in distribution in summer and winter seasons, and high in spring and autumn seasons. This was mainly related to the water vapor sources in the different seasons, and the meteorological conditions during precipitation. When δ^2H and $\delta^{18}O$ began depleting in May, it was likely due to the East Asian Monsoon, which begins that month, affecting precipitation on the plain, resulting in a relative depletion of the isotopes [31-32].

The relationship between the δ^2H and $\delta^{18}O$ of the precipitation constitutes the local meteoric water line (LMWL) of the plain (Fig. 3):

$$\delta^2H = 6.38\ \delta^{18}O + 0.72, \text{ VSMOW } (n = 254, R = 0.89)$$

This precipitation line deviates slightly from the global meteoric water line (GMWL: $\delta^2H = 8\ \delta^{18}O + 10$). This is because that the local circumfluent system has different water vapor sources and evaporation patterns from the global system [3,7]. The slop of LMWL is similar to the slopes of meteoric water lines for Shijiazhuang ($\delta^2H = 6.39\ \delta^{18}O - 3.75$, $R^2 = 0.88$) [33] and Zhengzhou ($\delta^2H = 6.48\ \delta^{18}O - 2.71$, $R^2 = 0.88$) [34], as well as the meteoric water lines of the adjacent GNIP stations in Yantai and Tianjin, which belong to the International Atomic Energy Agency ($\delta^2H = 6.29\ \delta^{18}O - 3.63$, $R^2 = 0.81$; $\delta^2H = 6.57\ \delta^{18}O + 0.31$, $R^2 = 0.94$). These all indicates that the precipitation sources of the plain were similar to that of these adjacent areas. Concurrently, the gradients of the meteoric water lines were lower than the GMWL's average value of 8, indicating that the precipitation process might be affected by secondary under-cloud evaporation. This caused partial fractionation of the δ^2H and $\delta^{18}O$, resulting in a reduction in the gradient of the precipitation line [3,8].

The d-excess of most terrestrial precipitation is close to 10‰ [35], which is mainly affected by the relative humidity of the surrounding air of the water vapor source. Analyzing the d-excess value can reveal the water vapor sources and the precipitation process, including the condensation, evaporation,

177 and sublimation of water vapor, and the recirculation of terrestrial water vapor [4,36]. The d-excess of
178 the precipitation of the Jiaolai Plain varied from -23.32‰ to 36‰ (average: 7.56‰) (Fig. 4). Most of the
179 d-excess values in the precipitation from October through April were higher than 10‰ (Fig. 4),
180 indicating the relative humidity of the surrounding air of the water vapor source was low. Meanwhile，
181 the $\delta^{2}H$ and $\delta^{18}O$ values of the precipitation during this period (spring, autumn, and winter) were mostly
182 located to the upper left of the LMWL (Fig. 3). These all indicated that the moisture sources of
183 precipitation on the plain from October through April were the water vapor controlled by the Westerlies
184 and local evaporation. There was also obvious recirculation of water vapor evaporated from the
185 terrestrial land [12,27,37-39]. Furthermore, most of the d-excess values of the precipitation from May to
186 September were less than 10‰ (Fig. 4), indicating that the humidity of the water vapor sources was
187 relatively high [40], and that possible sources of the precipitation were the adjacent coastal areas or the
188 low-latitude Pacific Ocean (with water vapor carried by the East Asian Monsoon) [41]. Meanwhile, the
189 $\delta^{2}H$ and $\delta^{18}O$ values of the precipitation during this period were mostly located to the lower right of the
190 LMWL (Fig. 3), indicating that summer precipitation on the plain was subjected to secondary
191 under-cloud evaporation [7,36]. Overall, the variations of d-excess of the precipitation on the plain were
192 obvious seasonal, the reason was mainly due to the different patterns of atmospheric circumfluence,
193 causing precipitation over the plain to have different water vapor sources during different periods [27].

194 **4.2 Environmental effects of the stable isotopes in precipitation**

195 4.2.1 The temperature effect

196 During the evaporation or condensation process, the fractionation intensities of $\delta^{2}H$ and $\delta^{18}O$ in
197 natural waterbodies are inversely proportional to the temperature, resulting in a linear relationship
198 between the values of $\delta^{2}H$ and $\delta^{18}O$ in the precipitation and air temperature. This is known as the
199 temperature effect [8]. The $\delta^{2}H$ and $\delta^{18}O$ in precipitation on the plain showed a strong seasonal variation

(Fig. 2). There was a gradual enrichment from January to May, followed by a gradual depletion from September to December. This means that, except for summer (June–August), the trends of the δ^2H and $\delta^{18}O$ of the precipitation were consistent with the temperature, indicating that the δ^2H and $\delta^{18}O$ of the precipitation on the plain evidenced a strong temperature effect. The temperature effect of the $\delta^{18}O$ of precipitation was significant ($p < 0.001$) during the sampling period (Fig. 5a), with the fitting equation being:

$$\delta^{18}O = 0.093T - 7.114 \ (n = 254, p < 0.001, R = 0.346)$$

The equation indicated that the $\delta^{18}O$ of the precipitation gradually enriched at the rate of 0.093‰/°C with rising temperatures, which was similar to the temperature effect at the adjacent Shijiazhuang [33]. In seasonal precipitation, the temperature effect of the $\delta^{18}O$ of precipitation exists in all seasons. The best-fit equations were significant ($p < 0.05$) in autumn and winter. Related studies have shown that the δ^2H and $\delta^{18}O$ in precipitation have a strong temperature effect in areas and during time periods that are controlled by the Westerlies, such as Delingha, Urumqi, and Zhangye in western China, and other arid regions in central Asia [4,27,42]. However, a strong precipitable amount effect counteracts the temperature effect in areas and during time periods that are controlled by the East Asian Monsoon, resulting in a weaker temperature effect [43-44]. This usually occurred near the equator and in southeastern China [4,27]. This further indicates that summer precipitation on the Jiaolai Plain might be controlled by the East Asian Monsoon and the ocean-evaporated water vapor that it carries, while precipitation in the other seasons is mainly controlled by the circumfluence of the Westerlies and the land-evaporated water vapor that they carry.

4.2.2 The amount effect

The amount of precipitation affects its isotopic composition. In many tropical as well as monsoon regions, an inverse relationship between precipitation amount and $\delta^{18}O$ of precipitation, called the

223 "amount effect," [8]. The amount effect of the $\delta^{18}O$ of precipitation was significant ($p < 0.05$) on the
224 plain during the sampling period (Fig. 6a), with the fitting equation being:

225 $$\delta^{18}O = -0.020\ P - 5.316\ (n = 254,\ p < 0.05,\ R = -0.144)$$

226 This is an indication that the $\delta^{18}O$ of the precipitation gradually depleted with an increasing amount of
227 precipitation, which might be due to the impact of the East Asian Monsoon [45]. Hong Kong and
228 Nanjing, which are affected by the monsoon, had obvious amount effects. Conversely, the amount effect
229 was relatively weak in Tianjin, and not significant in Qiqihar and the other inland areas [4,27].
230 According to the relationship between the $\delta^{18}O$ of the precipitation and the amount of precipitation in the
231 different seasons (Fig. 6), the amount effect did not exist in the $\delta^{18}O$ of the spring and winter
232 precipitation, but was significant ($p < 0.01$) in that of the summer and autumn precipitation.

233 Combining the above with the temperature effect on precipitation isotopes in different seasons on the
234 Jiaolai Plain (Fig. 5), the seasons with a significant amount effect (summer and autumn) were found to
235 not have any obvious temperature effect. However, the seasons with a non-significant amount effect
236 (spring and winter) had an obvious temperature effect. This indicates that the amount effect had
237 concealed or suppressed the temperature effect, although this phenomenon did not exist during snowfall
238 [26,40,46].

239 ### 4.2.3 The altitude effect

240 The altitude (elevation) effect refers to the phenomenon of topographic precipitation occurring when a
241 mass of water vapor is forced to rise from the ground surface in areas with relatively large topographic
242 undulations. The water vapor undergoes adiabatic condensation (through diffusion), causing the values
243 of $\delta^{18}O$ and $\delta^{2}H$ in the precipitation to decrease with increasing elevation [25]. According to the
244 relationship between the $\delta^{18}O$ of the precipitation and the altitude on the Jiaolai Plain (Fig. 7), the $\delta^{18}O$
245 of the precipitation had an inverse relationship with altitude during the sapling period, meaning that it

gradually depleted with altitude. This constitutes the altitude effect, although it was not significant (Fig. 7a). The altitude effect did not exist in the spring and autumn precipitation (Fig. 7b, 7d), while the altitude effect was present with respect to the summer and winter precipitation, but it was not significant (Fig. 7c, 7e). This might be related to the plain's relatively small altitudinal gradient, with an elevation difference of only 124.7 m between the highest and lowest points. For many studies, the altitudinal difference involved was greater than 3,000 m [7,12,31].

4.3 Precipitation sources of the Jiaolai Plain

The reanalysis data from NCEP/NCAR were used to obtain the wind speed and direction, relative humidity, and precipitable amount of the study area and its surrounding areas at the geopotential height of 850 hPa during the sampling period (October 2018 to September 2019) (Fig. 8, Fig. 9). The results show that air flows over the plain and surrounding areas were northwesterly from October to May of the following year, and were mainly controlled by the circumfluence of the Westerlies. From June to September, the air flows became southeasterly, and were mostly controlled by the East Asian Monsoon (Fig. 8). The main reason is that the East Asian Monsoon occurs after mid-May, and is jointly formed by a low-pressure center gradually appearing at 70°–80° E over the Qinghai–Tibet Plateau and a high-pressure center appearing over the North Pacific Ocean. The warm and wet water vapor formed over the Pacific Ocean is then transported across the East Asian continent [47]. After mid-September, a cold high-pressure center gradually appears over Mongolia, Siberia, and at 80°–90° E over the Qinghai–Tibet Plateau. The pressure gradient between Mongolia (high) and the Pacific Ocean (low) leads to the formation of the Winter Monsoon, which flows from west to east [27] and persists until May of the following year [48].

With the transitioning of the monsoons, the humidity and precipitable amount over the plain exhibited regular changes (Fig. 8, Fig. 9). Both humidity and precipitable amount presented an increasing trend

from January to August, going from below 30% to above 60% and from 7.5 to 40 kg/m^2, respectively. Next, these two variables showed a decreasing trend from August to December. During the period affected by the circumfluence of the Westerlies (October to May of the following year), the humidity and precipitable amount was less than 40% and 15 kg/m^2, respectively. These rose during the period controlled by the East Asian Monsoon (June to September), reaching 50% and 20 kg/m^2, respectively.

The precipitation isotopes of GNIP stations in different monsoon regions were selected for a comparative analysis to distinguish the water vapor sources of the precipitation on the plain more accurately (Fig. 1, Fig. 10, Fig. 11). The $\delta^{18}O$ of precipitation in Urumqi was positively correlated with temperature changes, and was characterized by a relative enrichment and depletion in summer and winter, respectively [49-50]. The precipitation in Hong Kong was mainly affected by oceanic water vapor carried by the East Asian Monsoon. The temperature was high in summer and the amount of precipitation was large. The main water vapor sources were the distant ocean regions, with the $\delta^{18}O$ of the precipitation being relatively depleted. The main water vapor sources of winter precipitation were the coastal waters and evaporation from local areas, and the precipitation was relatively enriched in $\delta^{18}O$ [27,51].

From October to May of the following year, the $\delta^{18}O$ of precipitation on the Jiaolai Plain exhibited a similar trend to that in Baotou, Shijiazhuang, Tokyo, and Nanjing (Fig. 10). The precipitation at the stations during this period was controlled by the Westerlies. The $\delta^{18}O$ of precipitation on the plain from June to September had a similar trend to that in Hong Kong, Tokyo, Nanjing, and Shijiazhuang. The East Asian Monsoon controlled the precipitation at the stations during this period. In contrast, the $\delta^{18}O$ of precipitation on the plain had the opposite trend to that in Urumqi during the period from June to September (Fig. 10a), where the precipitation during this period was controlled by the Westerlies [52]. The $\delta^{18}O$ of precipitation on the plain also had the opposite trend to that in Hong Kong from October to

May of the following year (Fig. 10b). During this period, the precipitation in Hong Kong was controlled by the East Asian Monsoon [27]. The results of comparing the $\delta^{18}O$ of precipitation at the stations were consistent with the NCEP/NCAR reanalysis data: the water vapor of precipitation on the Jiaolai Plain is controlled by the East Asian monsoon from June to September, and by the Westerlies from October to May.

During the period when the Westerlies were in control (October to May), the depletion of $\delta^{18}O$ in the precipitation at Urumqi and Qiqihar was at its highest (Fig. 10). This is because precipitation at these two stations was under the joint action of water vapor from both the Atlantic Ocean (carried by the circumfluence of the Westerlies) and the polar region. Water vapor condensed to form precipitation along the way, and was not well replenished by evaporation over land, leading to a depletion of $\delta^{18}O$ [52-53]. The d-excess in the precipitation isotopes at Urumqi was greater than 10, while that at Qiqihar was less than 10 (Fig. 11). This indicates that precipitation at Qiqihar contained a higher proportion of cold and wet water vapor from the Arctic Ocean, whereas that at Urumqi contained a greater proportion of water vapor evaporated from land [39,52-53].

The $\delta^{18}O$ of precipitation on the Jiaolai Plain and at the remaining stations (Baotou, Shijiazhuang, Tokyo, and Nanjing) was higher than at Urumqi and Qiqihar, and their d-excess values were greater than 10, indicating that the main water vapor source of precipitation over the plain was local evaporation during the period controlled by the Westerlies (October to May), and the impact of water vapor from the polar region was small. At the same time, the d-excess value of the plain was similar to that of Tokyo and Qiqihar during the period controlled by the East Asian Monsoon (June–September) (Fig. 11). Therefore, these three places share a similar water vapor source for their precipitation, namely water vapor evaporated from the adjacent Pacific Ocean, which has high levels of humidity [54].

Related studies have shown that the $\delta^{18}O$ value of typhoon-caused precipitation is significantly lower

than that of general precipitation events in summer, usually by 4‰-10‰ [56-58]. This may be related to various factors, including the cloud height and depth, lifetime and volume of the typhoon [58]. During this study's sampling period (October 2018 to September 2019), water vapor carried by Typhoon Lekima produced heavy precipitation over the plain from August 11–13, causing a change in the $\delta^{18}O$ of the precipitation, which ranged from -3.75‰ to -11.47‰ (average: -7.14‰). For the rest of August, which was unaffected by the typhoon, the $\delta^{18}O$ of the precipitation varied from -3.29‰ to -10.14‰ (average: -4.78‰). This proved that the precipitation isotopes were significantly depleted when affected by the typhoon weather system [59]. This is because the microphysical processes within the typhoon system caused the $\delta^{18}O$ of the precipitation to be significantly negative. This is known as the "cloud–rain zonal effect" [60-61].

5. Conclusion

The monthly $\delta^{2}H$ and $\delta^{18}O$ of precipitation on the Jiaolai Plain exhibited bimodal ("M"-shaped) variations, with the general pattern being low values in summer and winter, and high values in spring and autumn. The LMWL was $\delta^{2}H = 6.38\ \delta^{18}O + 0.72$. These two isotopes in the precipitation also displayed significant temperature and amount effects, but the altitude effect was not significant. The NCEP/NCAR reanalysis data were combined with our data for a comparative analysis of the isotopic characteristics and d-excess at several GNIP stations, which identified the water vapor sources for the plain. The water vapor source was controlled by the East Asian Monsoon from June to September, and was mainly evaporated from the adjacent Pacific Ocean. The source was controlled by the Westerlies from October to May, when it originated from the mixing of water vapor that had evaporated from large-scale waterbodies on land and atmospheric (upwind) water vapor. The impact of polar water vapor was small. The water vapor carried by Typhoon Lekima caused precipitation over the plain to be

significantly depleted in $\delta^{18}O$. The main reason was that the typhoon system has its own microphysical processes, which cause the "cloud–rain zonal effect" in which the $\delta^{18}O$ of the precipitation becomes significantly negative.

Acknowledgements

The study was supported by the National Natural Science Foundation of China (41877157); the Project supported by State Key Laboratory of Loess and Quaternary Geology (SKLLQG1904); the Science and technology support plan for Youth Innovation of colleges and universities of Shandong (2019KJH009); the Natural Science Foundation of Shandong Province (ZR2019BD005; ZR2019MD040); the Key Research and Development Plan of Shandong Province (2018GSF117021); and the Project supported by State Key Laboratory of Earth Surface Processes and Resource Ecology (2017-KF-15).

References

1. Trenberth, K.E., 1999. Atmospheric moisture recycling: Role of advection and local evaporation. Journal of Climate, 12(5): 1368-1381.
2. Puntsag, T., Mitchell, M.J., Campbell, J.L., Klein, E.S., Likens, G.E., Welker, J.M., 2016. Arctic Vortex changes alter the sources and isotopic values of precipitation in northeastern US. Scientific Reports, 6, 22647.
3. Clark, I.D., Fritz, P., 1997. Environmental Isotopes in Hydrogeology. Lewis Publishers.
4. Kong, Y.L., Pang, Z.H., 2016. A positive altitude gradient of isotopes in the precipitation over the Tianshan Mountains: Effects of moisture recycling and sub-cloud evaporation. Journal of Hydrology, 542: 222-230.
5. Aravena, R., Suzuki, O., 1990. Isotopic evolution of river water in the northern Chile Region. Water Resources Research, 26(12): 2887-2895.
6. Aggarwal, P.K., Alduchov, O.A., Froehlich, K.O., Araguás-Araguás, L.J., Sturchio, N.C., Kurita, N., 2012. Stable isotopes in global precipitation: A unified interpretation based on atmospheric moisture residence time. Geophysical Research Letters, 39, L11705.
7. Cui, B.L., Li, X.Y., 2015. Stable isotopes reveal sources of precipitation in the Qinghai Lake Basin of the northeastern Tibetan Plateau. Science of the Total Environment, 527-528: 26-37.
8. Dansgaard, W., 1964. Stable isotopes in precipitation. Tellus, 16: 436-468.
9. Gat, J.R., 1996. Oxygen and hydrogen isotopes in the hydrologic cycle. Annual Review of Earth and Planetary Sciences, 24(1): 225-262.
10. Rozanski, K., Araguás-Araguás, L., Gonfiantini, R., 1993. Isotopic patterns in modern global precipitation. Geophysical Monographs, 78, 1.
11. Uemura, R., Yonezawa, N., Yoshimura, K., Asami, R., Kadena, H., Yamada, K., Yoshida, N., 2012. Factors controlling isotopic composition of precipitation on Okinawa Island, Japan: implications for palaeoclimate reconstruction in the East Asian Monsoon Region. Journal of Hydrology, 475: 314-322.

12. Pang, Z.H., Kong, Y.L., Froehlich, K., Huang, T.M., Yuan, L.J., Li, Z.Q., Wang, F., 2011. Processes affecting isotopes in precipitation of an arid region. Tellus, 63(3): 352-359.
13. Wei, Z.W., Lee, X.H., Liu, Z.F., Seeboonruang, U., Koike, M., Yoshimura, K., 2018. Influences of large-scale convection and moisture source on monthly precipitation isotope ratios observed in Thailand, Southeast Asia. Earth and Planetary Science Letters, 488: 181-192.
14. Kong, Y.L., Wang, K., Li, J., Pang, Z.H., 2019. Stable Isotopes of Precipitation in China: A Consideration of Moisture Sources. Water, 11(6): 1239.
15. Fang, C.H., Liang, X.B., Liu, R.Z., 2012. Comparative analysis of marine economic difference based on geospatial gulfs: a case study of Liaodong Bay, Bohai Bay, Laizhou Bay. China Population, Resources and Environment, 22(2): 170-174. (In Chinese)
16. Yue, L.L., Gao, H.W., Liu, M.J., Zou, T., Chen, X.Y., 2016. The relationships between environment and economy of Qingdao City by using water quality parameters in Jiaozhou Bay. Marine Environmental Science, 35(1): 106-112. (In Chinese)
17. Gleeson, T., Befus, K.M., Jasechko, S., 2016. The global volume and distribution of modern groundwater. Nature Geoscience, 9:161-167.
18. Han, M., 1996. Relationship between the seawater intrusion and landforms in Laizhou Bay area. Oceanologia Et Limnologia Sinica, 27(4): 414-420. (In Chinese)
19. Li, D.G., Zhao, M.H., Han, M., Jian, G.X., Zhang, Z.L., 2000. A study of the shallowly-buried paleochannel zones in the south coast plain of the Laizhou Bay. Marine Geology & Quaternary Geology, 20(1): 23-28. (In Chinese)
20. Han, D.M., Song, X.F., Currell, M.J., et al., 2014. Chemical and isotopic constraints on evolution of groundwater salinization in the coastal plain aquifer of Laizhou Bay, China. Journal of Hydrology, 508(16): 12-27.
21. Hou, L.J., Li, H.L., Zheng, C.M., Ma, Q., Wang. C.Y., Wang. C.Y., Wang, X.J., Qu, W.J., 2016. Seawater-groundwater exchange in a silty tidal flat in the south coast of Laizhou Bay, China. Journal of Coastal Research, 74: 136-148.
22. Li, Y., Guo, J.J., Yang, S.H., Kong, X.F., 2007. Analysis on the development and evolvement of water table depression cone in Shandong Province. Ground Water, 29(4): 36-39. (In Chinese)
23. Meng, G.L., Han, Y.S., Wang, S.Q., Wang, Z.Y., 2002. Seawater intrusion types and regional divisions in the southern coast of Laizhou Bay. Chinese Journal of Oceanology and Limnology, 20(3): 277-284.
24. Ma, Q., Li, H.L., Wang, X.J., Wang, C.Y., Wan, L., Wang, X.S., Jiang, X.W., 2015. Estimation of seawater-groundwater exchange rate: case study in a tidal flat with a large-scale seepage face (Laizhou Bay, China). Hydrogeology Journal, 23: 265-275.
25. Xiao, B., Cui, B.L., Jiang, B.F., Li, D.S., Wang, Y., Zhao, T., 2019. Spatial and temporal variations of rainfall erosivity in different topographic regions of Shandong Province. Journal of Earth Environment, 10(3): 267- 280. (In Chinese)
26. Bortolami, G.C., Ricci, B., Susella, G.F., Zuppi, G.M., 1979. Hydrogeochemistry of the Corsaglia Valley, Maritime Alps, Piedmont, Italy. Journal of Hydrology, 44(1-2): 57-79.
27. Cook, P.G., Herczeg, A.L., 2000. Environmental tracers in subsurface hydrology. Dordrecht, the Netherlands: Kluwer Academic Publishers.
28. Tian, L.D., Yao, T.D., Sun, W.Z., Stievenard, M., Jouzel, J., 2001. Relationship between delta D and delta O-18 in precipitation from north to south of the Tibetan Plateau and moisture cycling. Science In China (Series D), 44(9): 789-796.
29. IAEA/WMO. Global network for isotopes in precipitation (EB/OL). http://isohis.iaea.org.
30. Araguás-Araguás, L., Froehlich, K., Rozanski, K., 1998. Stable isotope composition of precipitation over Southeast Asia. Journal of Geophysical Research-Atmospheres, 103(D22): 28721-28742.

31. Ma, J.Z., Zhang, P., Zhu, G.F., Wang, Y.Q., Edmunds, W.M., Ding, Z.Y., He, J.H., 2012. The composition and distribution of chemicals and isotopes in precipitation in the Shiyang River system, Northwestern China. Journal of Hydrology, 436: 92-101.
32. Ding, Y.H., Chan, J., 2005. The East Asian summer monsoon: An overview. Meteorology and Atmospheric Physics, 89: 117-142.
33. Wang, T., Zhang, J.R., Liu, X., Yao, L., 2013. Variations of stable isotopes in precipitation and water vapor sources in Nanjing area. Journal of China hydrology, 33(4): 25-31. (In Chinese)
34. Craig, H., 1961. Isotopic variation in meteoric waters. Science,133, 1702-1703.
35. Friedman, I., Smith, G.I., Gleason, J.D., Warden, A., Harris, J.M., 1992. Stable Isotope compositions of waters in southeastern California: Part 1, Modern precipitation. Journal of Geophysical Research, 97(5): 5795-5812.
36. Gat, J.R., Bowser, C.J., Kendall, C., 1994. The contribution of evaporation from the Great Lakes to the continental atmosphere: estimate based on stable isotope data. Geophysical Research Letters, 21(7): 557-560.
37. Froehlich, K., Kralik, M., Papesch, W., Rank, D., Scheifinger, H., Stichler, W., 2008. Deuterium excess in precipitation of Alpine regions-moisture recycling. Isotopes in Environmental and Health Studies, 44(1): 61-70.
38. Pang, Z.H., Kong, Y.L., Li, J., Tian, J., 2017. An isotopic geoindicator in the hydrological cycle. Procedia Earth and Planetary Science, 17: 534-537.
39. Wang, H.J., Zhang, J.L., Liu, Z.H., 2012. Indications of the hydrogen and oxygen isotope in precipitation for climate change in Huanglong, Sichuan. Carsologica Sinica, 31(3): 253-258. (In Chinese)
40. Yamanaka, T., Shimizu, R., 2007. Spatial distribution of deuterium in atmospheric water vapor: diagnosing sources and the mixing of atmospheric moisture. Geochimica et Cosmochimica Acta, 71(13): 3162-3169.
41. Zhu, Y.W., Zhang. F.P., Wang, H.W., Liu, X., 2017. Analysis on characteristics of stable hydrogen and oxygen isotopes in precipitation in Shijiazhuang. Shandong Agricultural Sciences, 49(5): 116-123. (In Chinese)
42. Yu, W.S., Yao, T.D., Tian, L.D., Ma, Y.M., Ichiyanagi, K., Wang, Y., Sun, W.Z., 2008. Relationships between delta O-18 in precipitation and air temperature and moisture origin on a south-north transect of the Tibetan Plateau. Atmospheric Research, 87(2): 158-169.
43. Zhao, P.P., Tan, L.C., Zhang, P; Wang, S.J., Cui, B.L., Li, D., Xue, G., Cheng, X., 2018. Stable Isotopic Characteristics and Influencing Factors in Precipitation in the Monsoon Marginal Region of Northern China. Atmosphere, 9(3): 97.
44. Li, Y.J., Zhang, M.J., Wang, S.J., Li, Z.Q., Wang, F.Q., 2011. Progress of the research of stable isotope in precipitation in China: a review. Journal of Glaciology and Geocryology, 33(3): 624-633. (In Chinese)
45. Chen, Z.X., Cheng, J., Guo, P.W., Lin, Z.Y., Zhang, F.Y., 2010. Distribution characters and its control factors of stable isotope in precipitation over China. Transactions of Atmospheric Sciences, 33(6): 667-679. (In Chinese)
46. Zhu, X.Q., Fan, T., Guan, W., 2013. The analysis of stable isotopes of precipitation in Kunming. Yunnan Geographic Environment Research, 25(5): 90-95. (In Chinese)
47. Ye, D.Z., Tao, S.Y., Li, M.C., 1958. The mutation phenomenon of the atmospheric circulation in June and October. Acta Meteorologica Sinica, 29(4): 249-263. (In Chinese)
48. He, J.H., Yu, J.J., Shen, X.Y., Gao, H., 2004. Research on mechanism and variability of east Asian monsoon. Journal of Tropical Meteorology, 20(5): 449-459. (In Chinese)
49. Tian, L.D., Yao, T.D., MacClune, K., White, J.W.C., Schilla, A., Vaughn, B., Vachon, R., Ichiyanagi, K., 2007. Stable isotopic variations in west China: a consideration of moisture sources. Journal of Geophysical Research, 112: D10112.
50. Yao, T.D., Masson-Delmotte, V., Gao, J., Yu, W., Yang, X., Risi, C., Sturm, C., Werner, M., Zhao, H., He, Y., Ren, W., Tian, L., Shi, C., Hou, S., 2013. A review of climatic controls on delta O-18 in precipitation over the Tibetan Plateau: Observations and simulations. Reviews of Geophysics, 51(4): 525-548.

51. Xie, L.H., Wei, G.J., Deng, W.F., Zhao, X.L., 2011. Daily delta O-18 and delta D of precipitations from 2007 to 2009 in Guangzhou, South China: Implications for changes of moisture sources. Journal of Hydrology, 400(2011): 477-489.
52. Feng, F., Feng, Q., Liu, X.D., Liu, W., Jin, S., 2013. Characteristics of delta O-18 and delta D in precipitation and moisture sources of Pailugou catchment in the Qilian Mountain. Journal of Desert Research, 37(5):997-1005. (In Chinese)
53. Li, X.F., Zhang, M.J., Ma, Q., Li, Y.J., Wang, S.J., Wang, B.L., 2012. Characteristics of stable isotopes in precipitation over Northeast China and its water vapor sources. Environmental Science, 33(9): 2924-2931. (In Chinese)
54. Kurita, N., Fujiyoshi, Y., Nakayama, T., Matsumi, Y., Kitagawa, H., 2015. East Asian Monsoon controls on the inter-annual variability in precipitation isotope ratio in Japan. Climate of the Past, 11: 339-353.
55. Lawrence, J.R., Gedzelman, S.D., 1996. Low stable isotope ratios of tropical cyclone rains. Geophysical Research Letters, 23(5): 527-530.
56. Ohsawa, S., Yusa, Y., 2000. Isotopic characteristics of typhonic rainwater: typhoons No.13 (1993) and no.6 (1996). Limnology, 1(2): 143-149.
57. Gedzelman, S., Lawrence, J., Gamache, J., Black, M., Hindman, E., Black, R., Dunion, J., Willoughby, H., Zhang, X.P., 2003. Probing hurricanes with stable isotopes of rain and water vapor. Monthly Weather Review, 131(6): 1112-1127.
58. Lawrence, J.R., Gedzelman, S.D., Zhang, X.P., Arnold, R., 1998. Stable isotope ratios of rain and vapor in 1995 hurricanes. Journal of Geophysical Research: Atmospheres, 103(D10): 11381-11400.
59. Huang, Y.M., Zhao, R.M., Song, X.F., He, Q.H., Yang, L., Zhang, X.P., 2019. Precipitation isotopes formed by typhoon “Haima” in the Dongting Lake Basin. Scientia Geographica Sinica, 39(7): 1184-1190. (In Chinese)
60. Xu, T., Cai, J.R., Sun, X.S., Cui, M.Y., Lei, G.L., Jiang, X.Y., 2018. A Tentative Study of “Cloudy and Rainy Area Effect” of the delta O-18 in the Precipitation of Typhoon “Dujuan”. Journal of Natural Resources, 33(12): 2238-2248. (In Chinese)
61. Xu, T., Sun, X.S., Hong, H., Wang, X.Y., Cui, M.Y., Lei, G.L., Gao, L., Liu, J., Lone, M.A., Jiang, X.Y., 2019. Stable isotope ratios of typhoon rains in Fuzhou, Southeast China, during 2013-2017. Journal of Hydrology, 570: 445-453.

Captions of Figures and Tables

Fig. 1. Location of the Jiaolai Plain and sites for sampling precipitation

Fig. 2. Contents of $\delta^{2}H$ and $\delta^{18}O$ in precipitation and temperature of the Jiaolai Plain

Fig. 3. The relationship between $\delta^{2}H$ and $\delta^{18}O$ of precipitation on the Jiaolai Plain

Fig. 4. Values of d-excess in precipitation on the Jiaolai Plain

Fig. 5. Temperature effect of $\delta^{18}O$ in precipitation on the Jiaolai Plain

Fig. 6. Amount effect of $\delta^{18}O$ in precipitation on the Jiaolai Plain

Fig. 7. Altitude effect of $\delta^{18}O$ in precipitation on the Jiaolai Plain

Fig. 8. Distributions of wind field (arrows) and humidity field (colors) at 850 hPa over the Jiaolai Plain and adjacent regions

Fig. 9. Distributions of precipitable water (colors) at surface level over the Jiaolai Plain and adjacent regions

Fig. 10. Seasonal variation of $\delta^{18}O$ in precipitation on the Jiaolai Plain and other stations derived from the GNIP network

Fig. 11. The d-excess in precipitation on the Jiaolai Plain and other stations derived from the GNIP network

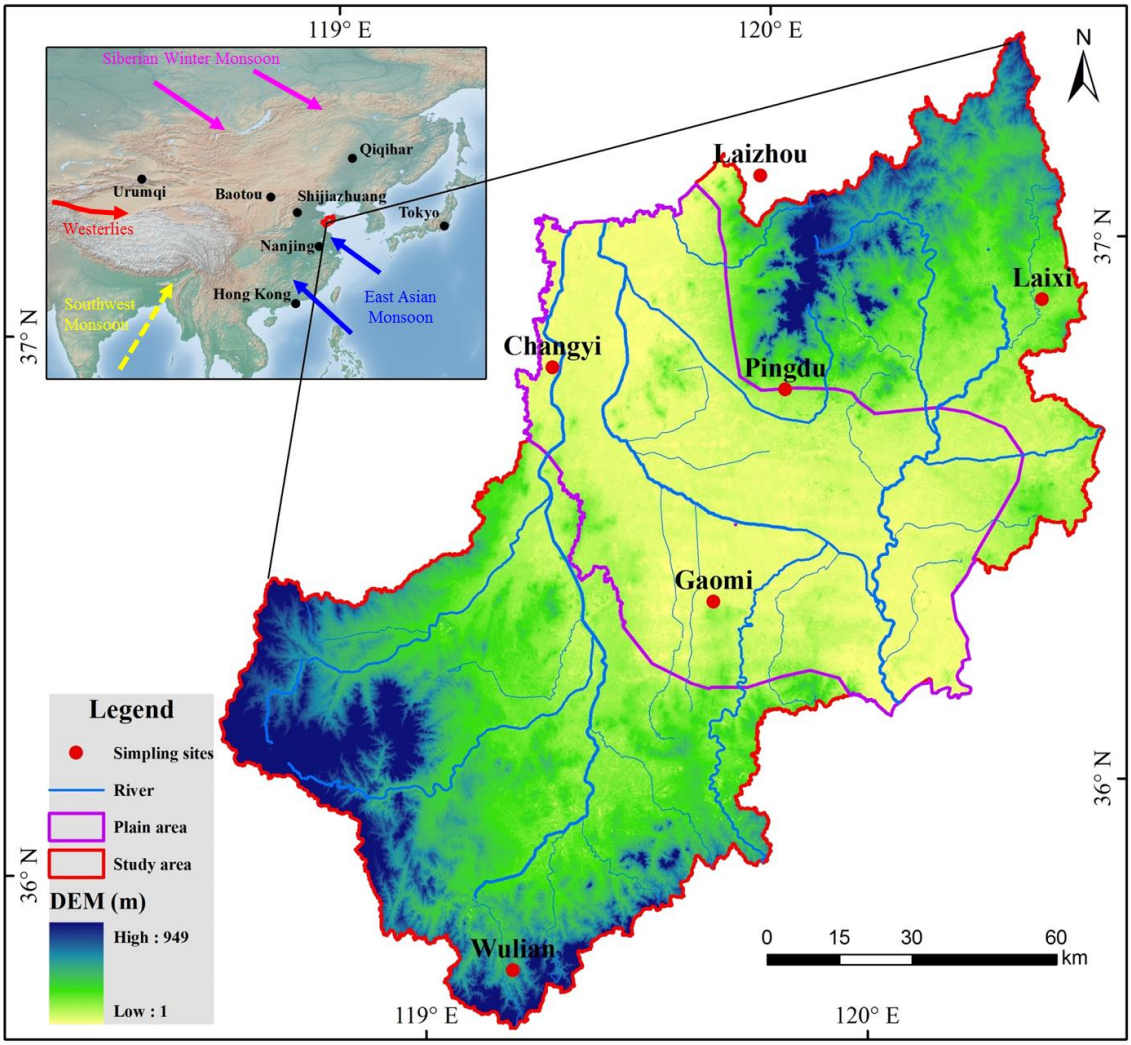

506

507 **Fig.1. Location of the Jiaolai Plain and sites for sampling precipitation**

508

509

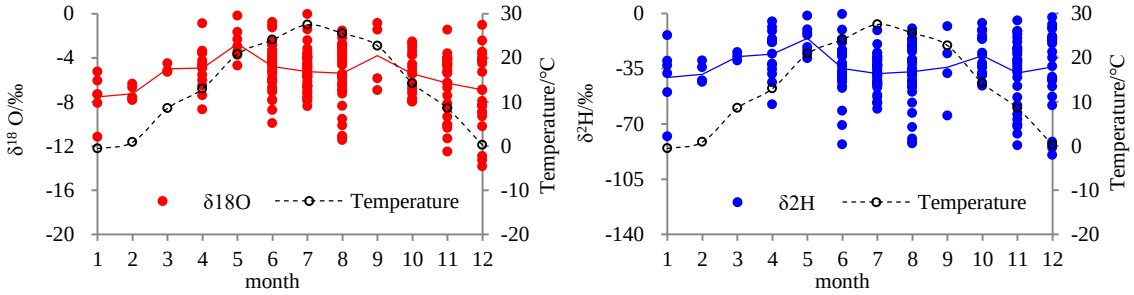

510

511 **Fig. 2. Contents of δ^2H and $\delta^{18}O$ in precipitation and temperature of the Jiaolai Plain**

512

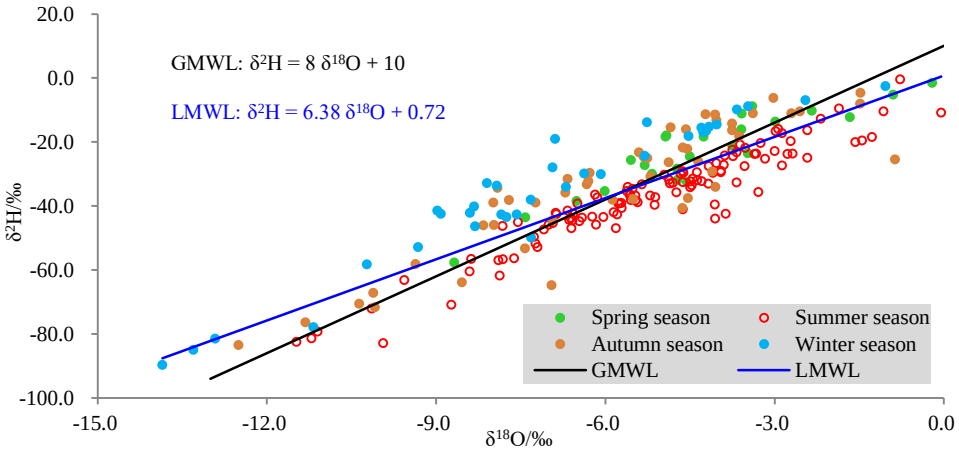

Fig. 3. The relationship between δ^2H and $\delta^{18}O$ of precipitation on the Jiaolai Plain

LMWL, Local Meteoric Water Line; GMWL, Global Meteoric Water Line

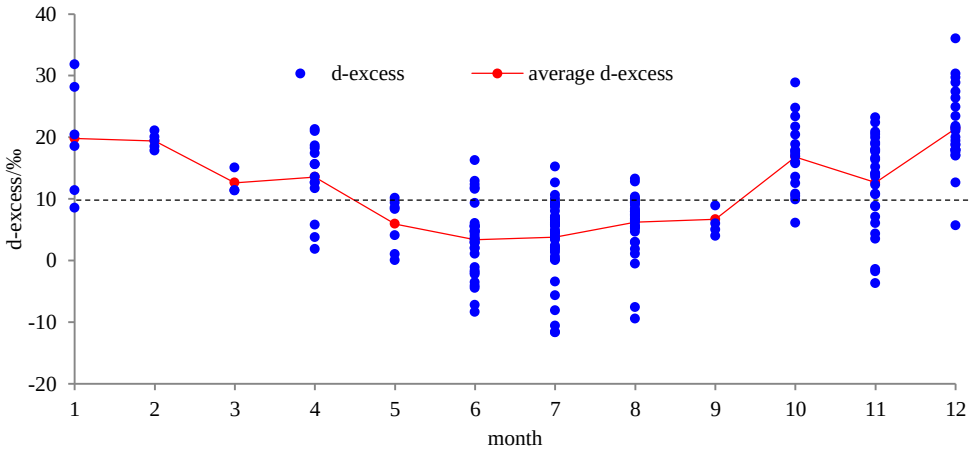

Fig. 4. Values of d-excess in precipitation of the Jiaolai Plain

522

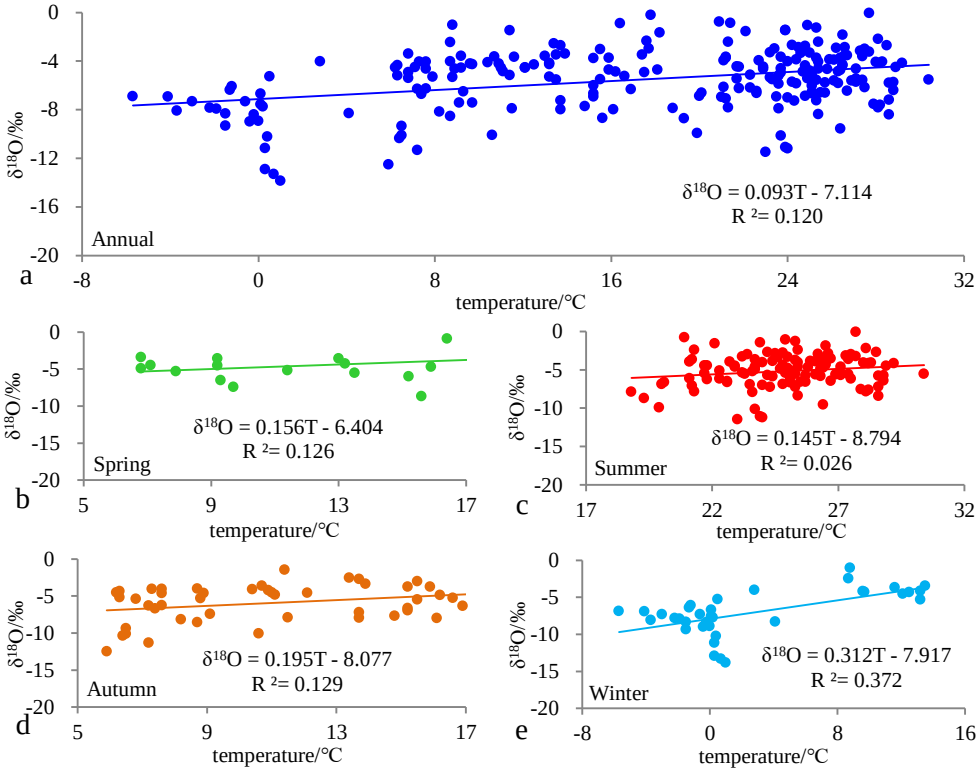

523

524 **Fig.5. Temperature effect of $\delta^{18}O$ in precipitation on the Jiaolai Plain**

525

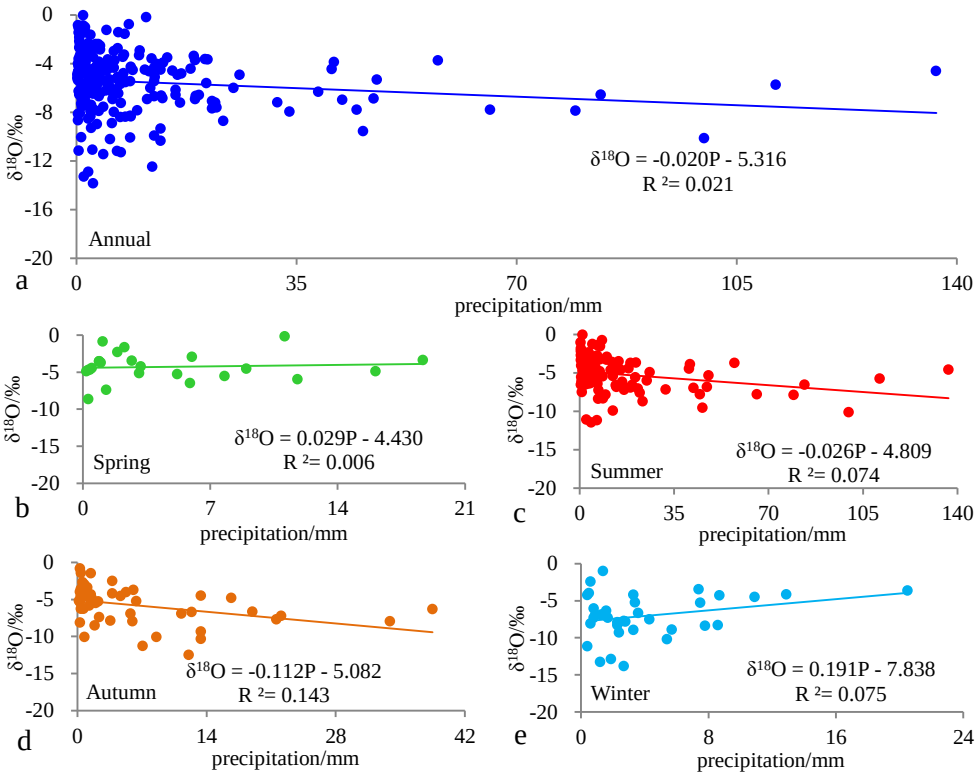

Fig.6. Amount effect of $\delta^{18}O$ in precipitation on the Jiaolai Plain

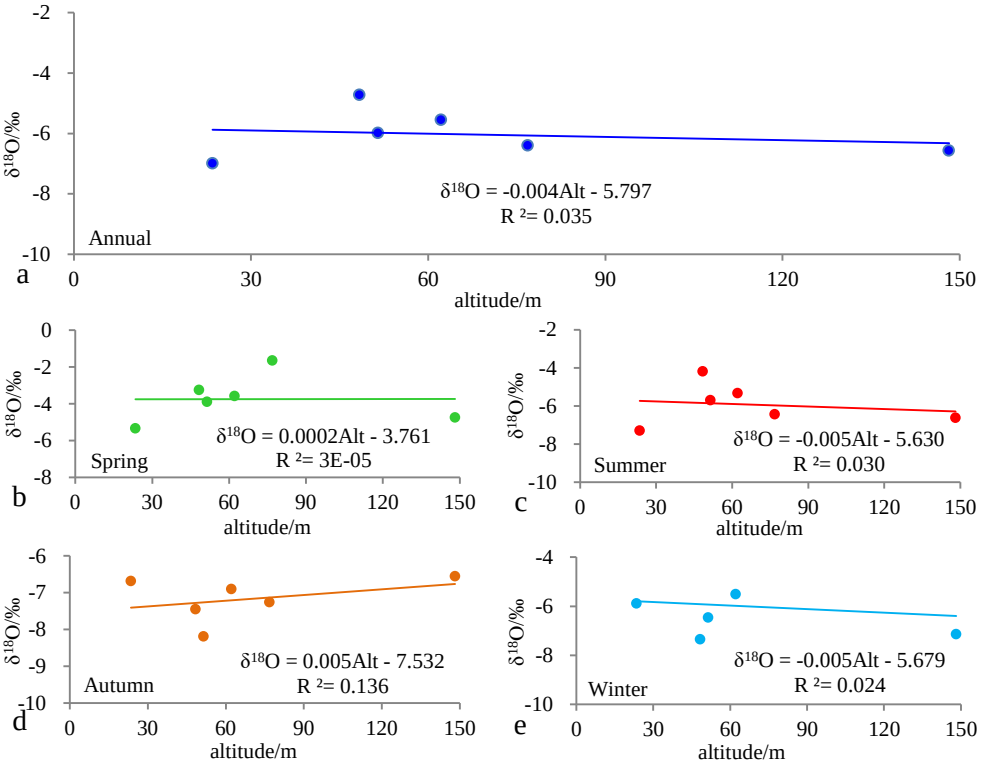

Fig.7. Altitude effect of $\delta^{18}O$ in precipitation on the Jiaolai Plain

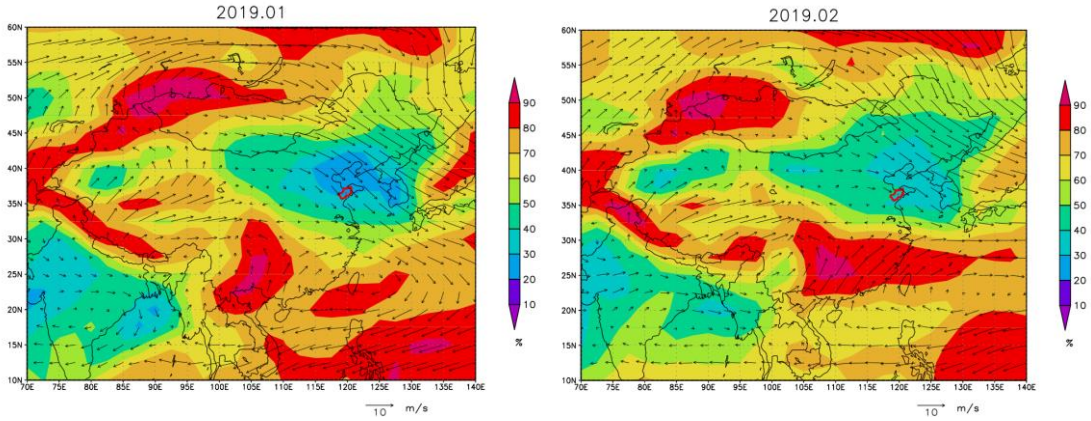

534

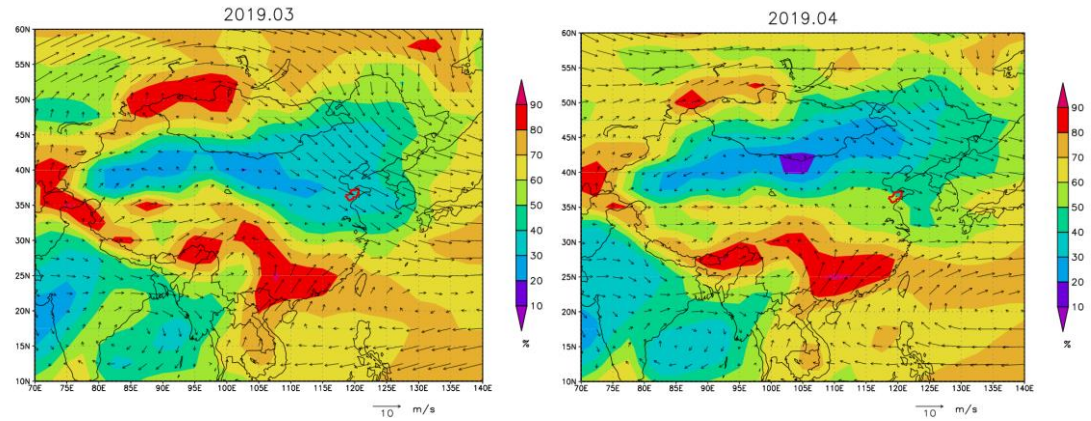

535

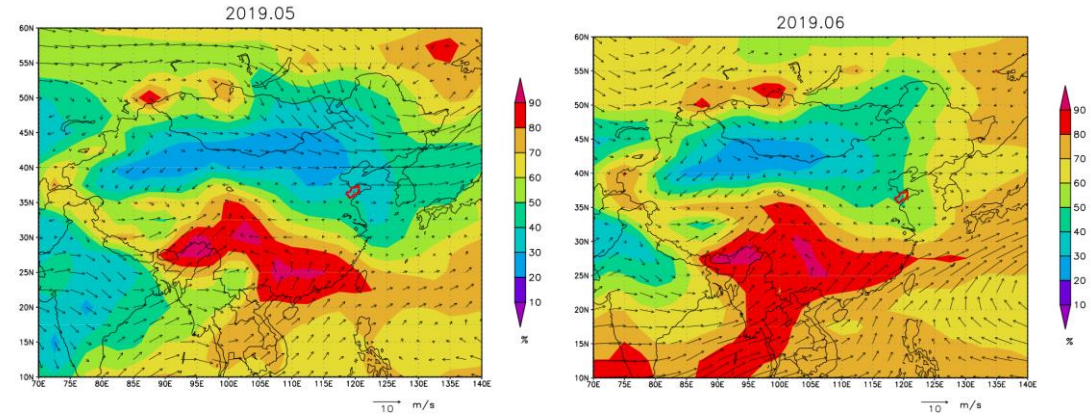

536

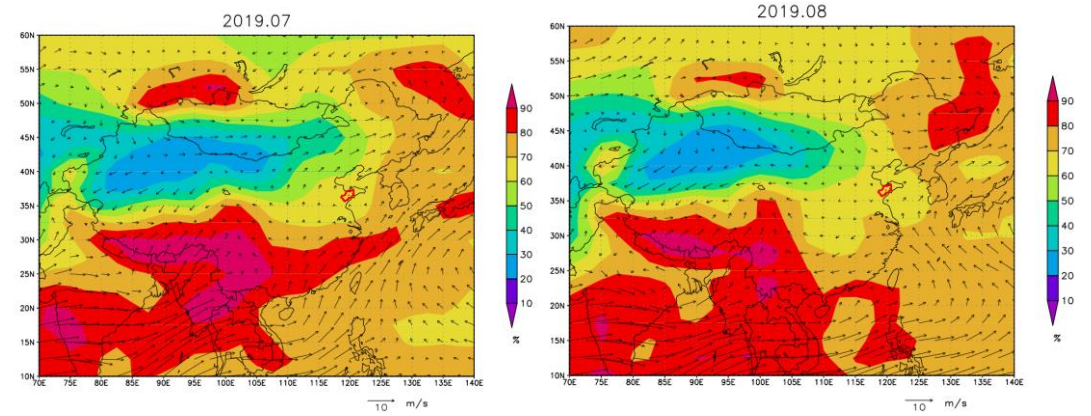

537

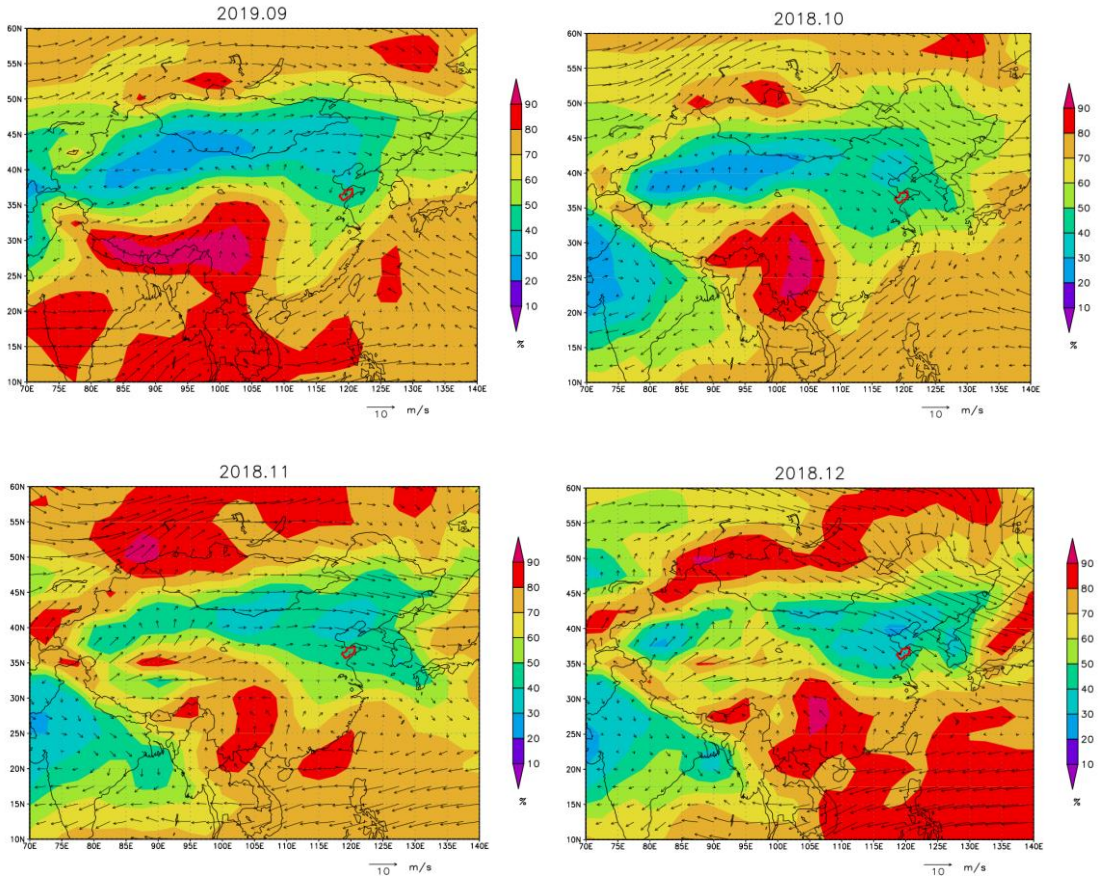

Fig.8. Distributions of wind field (arrows) and humidity field (colors) at 850hPa over the Jiaolai Plain and adjacent regions. Units of the color scale are % for humidity; the central red region is the study area.

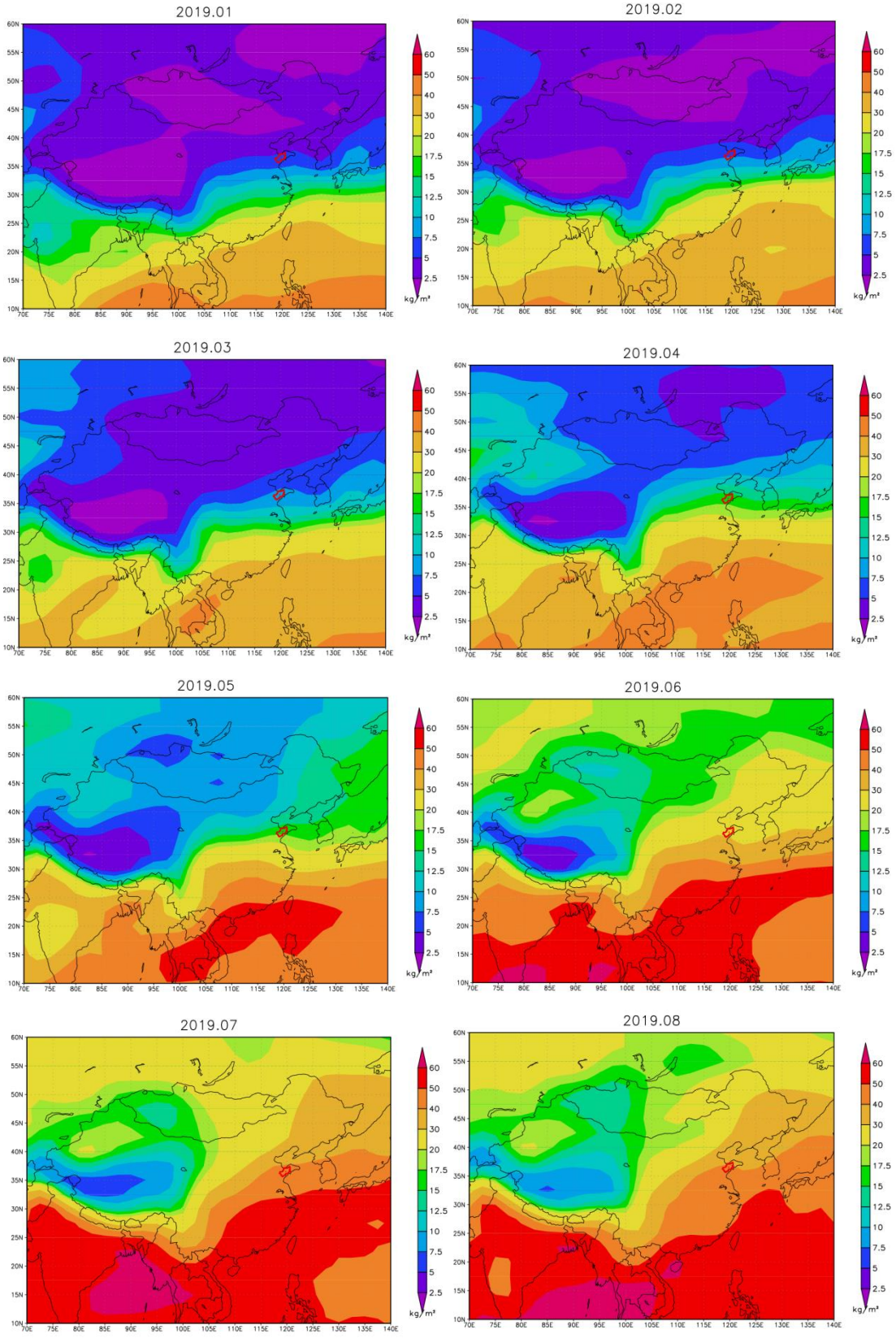
2019.01
2019.02
2019.03
2019.04
2019.05
2019.06
2019.07
2019.08
kg/m²

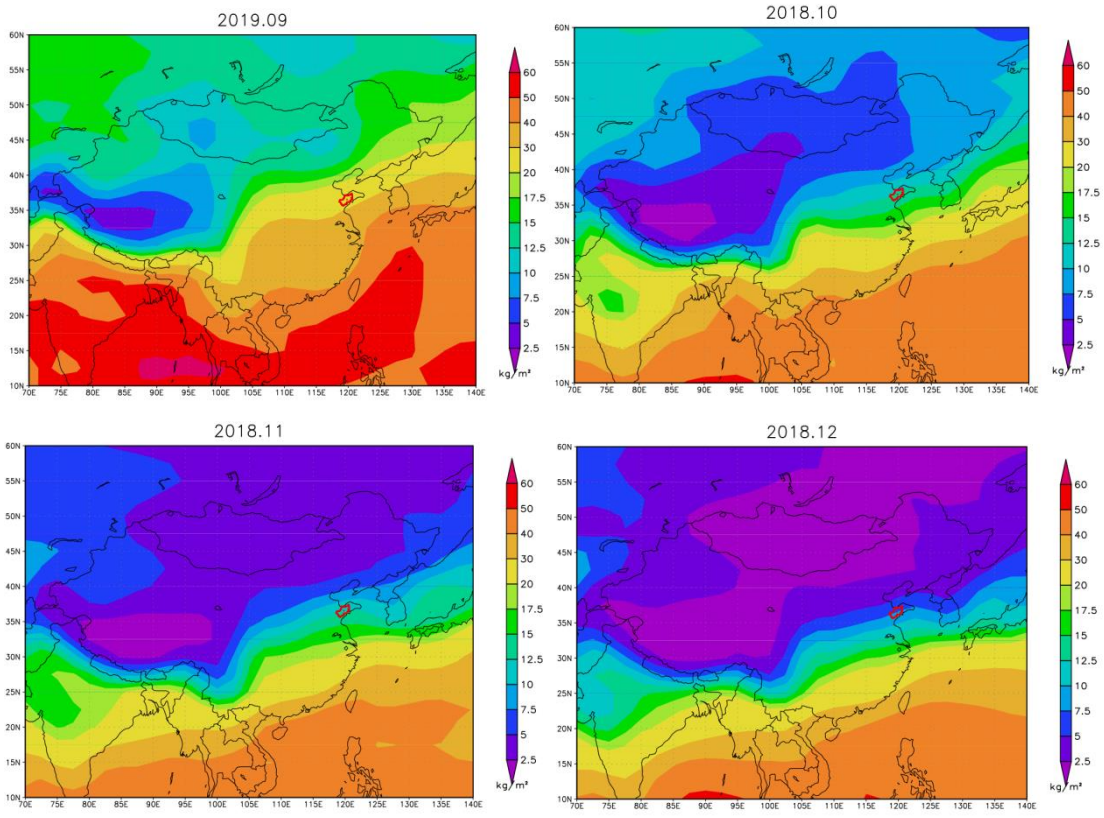

Fig. 9. Distributions of precipitable water (colors) at surface level over the Jiaolai Plain and adjacent regions. Units of the color scale are kg/m^2; the central red region is the study area.

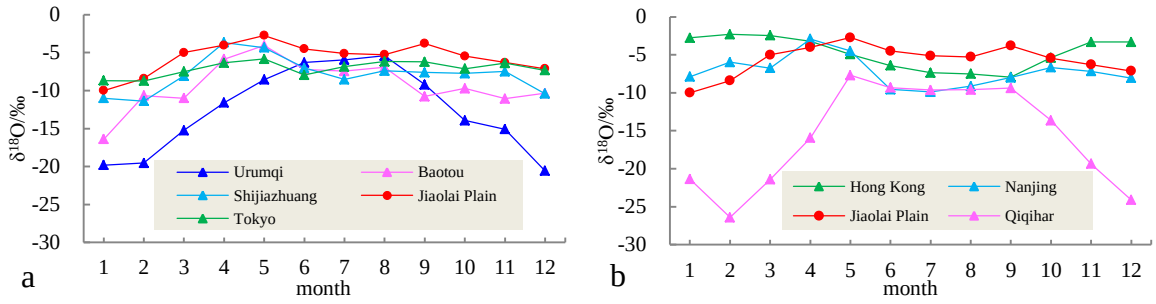

Fig. 10. Seasonal variation of $\delta^{18}O$ in precipitation on the Jiaolai Plain and other stations derived from GNIP network (a, transverse direction; b, longitudinal direction)

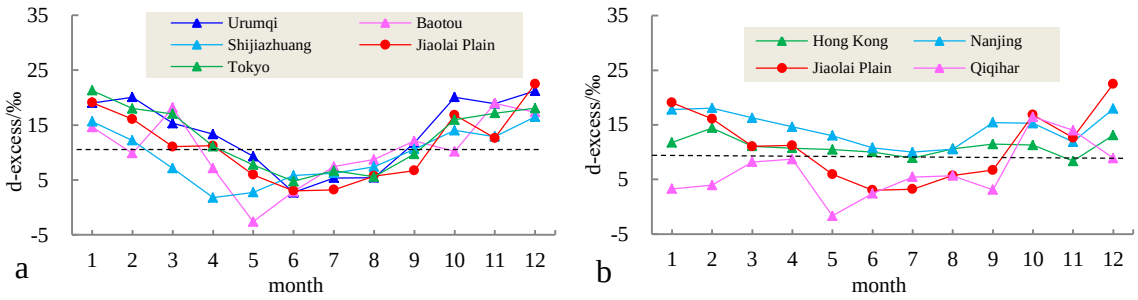

558

559 **Fig. 11. The d-excess in precipitation on the Jiaolai Plain and other stations derived from**

560 **GNIP network** (a, transverse direction; b, longitudinal direction)

561